Ann. der Physik 505, 308-319 (1993).

spin dynamics for 2d Heisenberg antiferromagnet with combined easy-plane and Dzyaloshinsky interactions.

On the spin dynamics of magnetic lipid layers of Manganese Stearate

A. R. Völkel
F. G. Mertens
Physics Institute, University of Bayreuth, W-8580 Bayreuth, Germany

A. R. Bishop
Theoretical Division and Center for Nonlinear Studies, LANL, Los Alamos, NM 87545, USA

G. M. Wysin
Physics Department, Kansas State University, Manhattan, Kansas 66506, USA

October 6, 1992

Abstract

We investigate the spin dynamics of the classical two-dimensional easy-plane Heisenberg antiferromagnet with an additional Dzyaloshinsky interaction, which serves as a simple model for Langmuir-Blodgett films of $Mn(C_{18}H_{35}O_2)_2$. By mapping the system onto a pure easy-plane model we discuss the corresponding spin wave and vortex dynamics. The additional Dzyaloshinsky interaction forces all spins to cant in a certain direction, which is the same for neighboring spins on different sublattices. This canting causes the presence of a second spin wave peak in the dynamical in-plane correlation function below the Kosterlitz-Thouless transition temperature T_{KT} and a second vortex central peak above T_{KT}. Using a vortex gas approach we explicitly calculate the contribution of the free vortices to several dynamical correlation functions. These results are compared to a combined Monte Carlo-Molecular Dynamics simulation on square lattices with different sizes. We also discuss the relevance of this simple model for describing the spin dynamics of $Mn(C_{18}H_{35}O_2)_2$.

Keywords: antiferromagnet, weak ferromagnetism, vortex dynamics

1 Introduction

In recent years increased attention has been paid to two-dimensional (2d) magnetic systems based on a wide class of newly available materials such as (i) layered magnets [1] (e.g. $BaNi_2(PO_4)_2$) [2,3], K_2CuF_4 [4], or $(CH_3NH_3)_2CuCl_4$ [5]), (ii) $CoCl_2$ intercalated graphite compounds [6], and (iii) magnetic Langmuir Blodgett films like the manganese stearate $Mn(C_{18}H_{35}O_2)_2$ [7,8,9]. All of the above listed materials have an easy-plane (XY) symmetry, i.e. the spins tend to lie mainly within a plane. A simple model for these systems is described by the Heisenberg Hamiltonian

$$\mathcal{H} = J \sum_{<i,j>} \left(S_i^x S_j^x + S_i^y S_j^y + \lambda S_i^z S_j^z \right) \tag{1}$$

with

$$0 \leq \lambda < 1 \tag{2}$$

and the $< i, j >$ denoting nearest neighbor pairs. As was shown by Kosterlitz and Thouless [10] and Berezinsky [11], these types of magnets undergo a phase transition due to the unbinding of pairs of topological excitations, namely vortices, at T_{KT}.

In previous work we have studied the dynamics of the unbound vortices just above the transition temperature T_{KT} for both ferromagnetic (FM, $J < 0$) [12,13,14,15,16,17] and antiferromagnetic (AFM, $J > 0$) [17,18] exchange couplings. There we assumed a dilute gas of weakly interacting vortices to calculate the contributions of the freely moving vortices to the dynamical correlation functions. This approach turned out to be quite successful in a temperature range of $T_{KT} \lesssim T \lesssim 1.25 T_{KT}$ for $\lambda = 0$, before a more diffusive spin dynamics becomes dominant. This temperature range is reduced for $\lambda > 0$, where a crossover to isotropic behavior can be observed (cf. [4]) at a certain temperature T_c ($T_c \approx 1.14 T_{KT}$ for $\lambda = 0.8$ [17]). These analytic results can be compared with numerical Monte Carlo-Molecular Dynamics (MC-MD) simulations in the above discussed temperature regimes. By analyzing the results of the computer experiments we obtain values for the vortex correlation length ξ and the vortex average velocity $\bar{u}$ – the two parameters of our vortex-gas approach. Comparison with experiments is complicated: The materials of the classes (i) and (ii) (see above) are only quasi-two-dimensional magnets, i.e. they have a small interlayer coupling which becomes dominant for low temperatures leading to a three-dimensional ordering just above T_{KT} – therefore decreasing the regime where we expect to observe clear vortex signatures in the dynamical correlation functions and, moreover, introducing competing three-dimensional spin fluctuations.

These difficulties can, in principle, be overcome by using the AFM substance $Mn(C_{18}H_{35}O_2)_2$ which can be produced as a monolayer by using the Langmuir Blodgett technique. However, measurements on such single layers promise to be quite difficult due to the low spin density in the system, and so far only

a few experiments were made on this material, mostly on stacks of those layers. EPR measurements at high temperatures [7] exhibit a characteristic anisotropy of the line width as function of the direction of the applied magnetic field, confirming the 2d character of the magnetic layers [19]. Furthermore, one finds an AFM coupling between the Mn^{2+} ions by analyzing the susceptibility χ which shows good Curie-Weiß behavior in these experiments. These properties of χ are verified by SQUID measurements [8,9], however, only for $T_1 \gtrsim 15K$. Below T_1 the susceptibility increases stronger until it reaches a maximum at $T \cong 0.5K$. This increase in χ can be explained by an anisotropic exchange interaction between the spins which becomes relevant in this temperature range. Below $T \cong 0.5K$ the system probably locks into an ordered phase.

Pomerantz [7] concluded, by comparing low-temperature spin wave dispersions with calculations of Yoshida and Saiki [20], that $Mn(C_{18}H_{35}O_2)_2$ can be well described by an isotropic Heisenberg Hamiltonian with a very weak Ising anisotropy and an asymmetric spin interaction as discussed by Dzyaloshinsky [21] and Moriya [22]

$$\mathcal{H} = E\,\mathbf{e}_z \cdot \sum_{<i,j>} \mathbf{S}_i \times \mathbf{S}_j, \tag{3}$$

where E is the strength of this interaction, $\mathbf{e}_z$ is the unit vector perpendicular to the easy-plane and "$\times$" denotes the vector cross product.

In the following we discuss a Heisenberg model of type (1) with an additional Dzyaloshinsky interaction (3). The additional Ising anisotropy is very weak for $Mn(C_{18}H_{35}O_2)_2$ and plays a dominant role only at temperatures $T \lesssim 0.5K$, where it leads to an ordered state. However, for higher temperatures we expect that the systems shows mainly XY-type behavior on which we will focus in this manuscript and which is well described by our model. First (Sec. 2) we show that the combined Hamiltonian can be mapped again onto the pure AFM Heisenberg model as described by Eqn. (1), but with canted spins and renormalized parameters (which enhance the easy-plane nature of the system). The calculation of various dynamical correlation functions is then a straightforward extension of our previous results. In Sec. 3 we compare the analytic results with Monte Carlo - Molecular Dynamics (MC-MD) simulations. Sec. 4 contains a short summary.

2 Theory

We investigate the following Hamiltonian

$$\mathcal{H} = J \sum_{<i,j>} \left(S_i^x S_j^x + S_i^y S_j^y + \lambda S_i^z S_j^z\right) + E\,\mathbf{e}_z \cdot \sum_{<i,j>} \mathbf{S}_i \times \mathbf{S}_j. \tag{4}$$

Here the i's label only the sites of the even, and j's only the sites of the odd, sublattice – this convention guarantees that the sign of the Dzyaloshinsky interaction is correct on each bond (i.e. the sign on neighboring bonds along a given direction is alternating). We consider (4) to be classical and treat the spins $\mathbf{S}_l = (S_l^x, S_l^y, S_l^z)$ as fixed length vectors which can rotate freely around their lattice sites. This corresponds to the limit $S \to \infty$, but the approximation is already very good for $S = \frac{5}{2}$, the value of the spins of the Mn^{2+} ions in $Mn(C_{18}H_{35}O_2)_2$.

The Hamiltonian (4) can be transformed to form (1) by rotating all the spins on the even (odd) sublattice by an angle of $-\frac{\epsilon}{2}$ ($\frac{\epsilon}{2}$):

$$\tilde{\mathbf{S}}_i = \begin{pmatrix} \cos\frac{\epsilon}{2} & -\sin\frac{\epsilon}{2} & 0 \\ \sin\frac{\epsilon}{2} & \cos\frac{\epsilon}{2} & 0 \\ 0 & 0 & 1 \end{pmatrix} \mathbf{S}_i \tag{5}$$

$$\tilde{\mathbf{S}}_j = \begin{pmatrix} \cos\frac{\epsilon}{2} & \sin\frac{\epsilon}{2} & 0 \\ -\sin\frac{\epsilon}{2} & \cos\frac{\epsilon}{2} & 0 \\ 0 & 0 & 1 \end{pmatrix} \mathbf{S}_j, \tag{6}$$

where ϵ is defined by

$$\tan\epsilon = e = \frac{E}{J}. \tag{7}$$

With the renormalized parameters $\tilde{J} = \frac{J}{\cos\epsilon}$ and $\tilde{\lambda} = \lambda\cos\epsilon$ we finally arrive at

$$\mathcal{H} = \tilde{J} \sum_{<i,j>} \left(\tilde{S}_i^x \tilde{S}_j^x + \tilde{S}_i^y \tilde{S}_j^y + \tilde{\lambda} \tilde{S}_i^z \tilde{S}_j^z \right). \tag{8}$$

Because of $\tilde{\lambda} < \lambda$ one can see that the additional Dzyaloshinsky interaction enhances the easy-plane character of the system (and especially it leads to an easy-plane sysmmetry for an isotropic ($\lambda = 1$) Heisenberg model). It should also be emphasized that, although this additional asymmetric interaction forces all the spins to cant in a certain direction, it does not destroy the in-plane rotational symmetry in contrast, e.g., to an in-plane magnetic field.

2.1 Spin waves

Starting from a Néel state in the spin variables $\tilde{\mathbf{S}}_i$ and $\tilde{\mathbf{S}}_j$ we can perform a linear spin wave calculation at low temperatures [23,17] and obtain

$$\mathcal{H} = \sum_{\mathbf{q}} \left(\hbar\omega_+(\mathbf{q}) \alpha_{\mathbf{q}}^\dagger \alpha_{\mathbf{q}} + \hbar\omega_-(\mathbf{q}) \beta_{\mathbf{q}}^\dagger \beta_{\mathbf{q}} \right) \tag{9}$$

with the two dispersion relations

$$\omega_\pm(\mathbf{q}) = \tilde{J} S z \sqrt{\left(1 \mp \gamma(\mathbf{q})\right)\left(1 \pm \tilde{\lambda}\gamma(\mathbf{q})\right)}. \tag{10}$$

These are the same dispersions as for the pure AFM model, but with the renormalized parameters ($\tilde{J}$, $\tilde{\lambda}$) and

$$\gamma(\mathbf{q}) = \frac{1}{z}\sum_{j=1}^{z} e^{i\mathbf{q}\cdot\rho_j}, \tag{11}$$

where the ρ_j are the vectors to the z nearest neighbors on the lattice. $\alpha_{\mathbf{q}}^{\dagger}$ and $\alpha_{\mathbf{q}}$ ($\beta_{\mathbf{q}}^{\dagger}$ and $\beta_{\mathbf{q}}$) are the creation and annihilation operators for spin waves of the dispersion branch $\omega_+(\mathbf{q})$ ($\omega_-(\mathbf{q})$).

The calculation of the spin wave contributions to the dynamical correlation functions $S^{\alpha\alpha}(\mathbf{q},\omega)$, $\alpha = x, y, z$ is also straightforward (within this linear spin wave approximation) and, due to the canting of the spins, we observe in the in-plane correlations, besides the peak corresponding to the ω_--dispersion (with an amplitude proportional to $\cos^2\frac{\epsilon}{2}$), also a peak corresponding to the ω_+-dispersion ($\propto \sin^2\frac{\epsilon}{2}$). Within this ansatz these two peaks should be visible throughout the whole Brillouin zone, and each of them has a distinct maximum of its intensity at the $\mathbf{q}$-value where the corresponding spin wave frequency becomes zero. For the out-of-plane correlations we find no difference from the pure AFM model, i.e. there is only one spin wave peak in $S^{zz}(\mathbf{q},\omega)$ following the ω_+-dispersion.

2.2 Vortices

To determine single vortex solutions from (9) we first derive the equations of motion. It is convenient to use angular variables first introduced by Mikeska [24]:

$$\tilde{\mathbf{S}}_i = S\left(\cos(\Phi_i+\phi_i)\cos(\Theta_i+\theta_i), \sin(\Phi_i+\phi_i)\cos(\Theta_i+\theta_i), \sin(\Theta_i+\theta_i)\right) \tag{12}$$

$$\tilde{\mathbf{S}}_j = -S\left(\cos(\Phi_j-\phi_j)\cos(\Theta_j-\theta_j), \sin(\Phi_j-\phi_j)\cos(\Theta_j-\theta_j), \sin(\Theta_j-\theta_j)\right); \tag{13}$$

here the capital angles Φ_l and Θ_l describe the local AFM alignment, while the small angles ϕ_l and θ_l describe deviations from it. Furthermore, we will perform these calculations in the continuum limit using the angular fields $\Phi(\mathbf{r})$, $\phi(\mathbf{r})$, $\Theta(\mathbf{r})$, and $\theta(\mathbf{r})$, which are, on the lattice sites l, equivalent to the variables Φ_l, ϕ_l, Θ_l, and θ_l, respectively. The results for the vortex solutions are exactly the same as in the pure AFM model [17,18]. Namely, we obtain either an "in-plane vortex" (IPV) for $\tilde{\lambda} < \lambda_c \approx 0.71$ with a static structure which is purely in-plane, or an "out-of-plane vortex" (OPV) for $\tilde{\lambda} > \lambda_c$ with a well-localized out-of-plane shape around its center. However, the angle $\phi(\mathbf{r})$ has now a finite offset due to the canting of the spins, i.e.

$$\phi(\mathbf{r}) = -\frac{\epsilon}{2} + \tilde{\phi}(\mathbf{r}), \tag{14}$$

where $\tilde{\phi}(\mathbf{r})$ is the corresponding solution of the pure AFM model. Therefore, for a single static vortex all the spins are rotated about $\frac{\epsilon}{2}$ either towards or away from the vortex center. As was already discussed in [17,18] the static structures are described by the angles $\Phi(\mathbf{r})$ (plus the offset $-\frac{\epsilon}{2}$) and $\Theta(\mathbf{r})$ ($\Theta(\mathbf{r})$ is

nonzero only for $\tilde{\lambda} > \lambda_c$), while the deviations from these structures due to a finite velocity u are described only by $\tilde{\phi}(\mathbf{r})$ and $\theta(\mathbf{r})$.

The results for the static vortex structure as well as for the spin wave dispersions (10) are well verified by numerical simulations (c.f. Fig 1 and Sec. 3, respectively).

For the dynamic out-of-plane correlations we find no impact of the Dzyaloshinsky interaction on $S^{zz}(\mathbf{q},\omega)$, and we obtain a small Gaussian CP at $\mathbf{q} = (0,0)$ for all possible $\tilde{\lambda}$, and a dominant Gaussian CP at $\mathbf{q} = (\pi,\pi)$ for $\tilde{\lambda} > \lambda_c$.

To calculate the dynamical in-plane correlation function we start with

$$S_{ij}^{xx}(t) =< \left[\tilde{S}_i^x(t)\right]^* \tilde{S}_j^x(t) > . \tag{15}$$

If we use the fact that $\tilde{\phi}(\mathbf{r})$, $\theta(\mathbf{r})$, $\Theta(|\mathbf{r}| > r_v) << 1$ ($r_v = \frac{1}{2}\sqrt{\frac{\tilde{\lambda}}{1-\tilde{\lambda}}}$ is the vortex core radius for OPV's) and by decoupling the Φ-correlations (which are mainly given by spin flips at lattice sites, as the vortices pass by) Eqn. (15) can be rewritten as

$$\begin{aligned} S_{ij}^{xx}(t) =& < e^{i\mathbf{K}^0\cdot\mathbf{r}} \cos\Phi(\mathbf{r},t)\cos\Phi(0) > \left((1-A)\cos^2\frac{\epsilon}{2} + B\sin^2\frac{\epsilon}{2}\right) \\ &+ < \sin\Phi(\mathbf{r},t)\sin\Phi(0) > \left((1-A)\sin^2\frac{\epsilon}{2} + B\cos^2\frac{\epsilon}{2}\right) \quad , \end{aligned} \tag{16}$$

with the abbreviations $A =< \Theta^2(\mathbf{r}) + \theta^2(\mathbf{r}) + \phi^2(\mathbf{r}) >$, $B =< \phi(\mathbf{r},t)\phi(0) >$, and $\mathbf{K}^0 = (\mu\pi,\nu\pi)$, $\mu,\nu = \pm 1, \pm 3, \pm 5, \ldots$. By Fourier transforming (16) we finally obtain, in zeroth order,

$$S^{xx}(\mathbf{q},\omega) = S_{old}^{xx}(\mathbf{K}^0 - \mathbf{q},\omega)\cos^2\frac{\epsilon}{2} + S_{old}^{xx}(\mathbf{q},\omega)\sin^2\frac{\epsilon}{2}, \tag{17}$$

where [12]

$$S_{old}^{xx}(\mathbf{q},\omega) = \frac{S^2}{2\pi^2}\frac{\gamma^3\xi^2}{\{\omega^2 + \gamma^2[1+(\xi\mathbf{q})^2]\}^2}, \tag{18}$$

$\gamma = \frac{\sqrt{\pi}\bar{u}}{2\xi}$, and ξ and $\bar{u}$ are the vortex correlation length and average velocity, respectively. The first term in (17) represents a squared Lorentzian CP at $\mathbf{q} = (\pi,\pi)$ (also present in the pure AFM model). The second term is a similar peak at $\mathbf{q} = (0,0)$ which reflects the local ferromagnetic moment introduced by the canting of the spins due to the Dzyaloshinsky interaction.

In the above derivation we have neglected any in-plane spin wave contributions, though there are expected to be spin fluctuations around $\omega = 0$ (even for finite values of $\mathbf{q}$) due to the sudden softening of the in-plane spin stiffness constant for $T \gtrsim T_{KT}$ ("universal jump" [25]). Furthermore, we have neglected any internal vortex structure in deriving $S_{old}^{xx}(\mathbf{q},\omega)$. Thus, we expect our result to be valid only close to the points $\mathbf{q} = (0,0)$ and $\mathbf{q} = (\pi,\pi)$.

3 Comparison with simulations

The results discussed above will now be compared to a combined MC-MD simulation on square lattices with different sizes from 40x40 to 100x100. The MC algorithm is used to bring the system into thermal equilibrium at a given temperature. From these configurations we use a fourth-order Runge Kutta method to integrate the equations of motion,

$$\dot{\mathbf{S}}_l = \mathbf{S}_l \times \mathbf{F}_l, \tag{19}$$

with the effective magnetic field

$$\mathbf{F}_l = -\frac{\delta H}{\delta \mathbf{S}_l} = J \sum_{\epsilon} ((S^x_\epsilon - b_\epsilon S^y_\epsilon)\mathbf{e}_x + (S^y_\epsilon + b_\epsilon S^x_\epsilon)\mathbf{e}_y + \lambda S^z_\epsilon \mathbf{e}_z), \tag{20}$$

from which we can derive the dynamical correlation functions by Fourier transformation of the spin-spin corelations ($\alpha = x, y, z$)

$$S^{\alpha\alpha}(\mathbf{q},\omega) = \int_{-\infty}^{\infty} \frac{\mathrm{d}t}{2\pi} \sum_{i,j} e^{i[\mathbf{q}\cdot(\mathbf{r}_i - \mathbf{r}_j) - \omega t]} < [S^\alpha_i(t)]^* \, S^\alpha_j(0) > . \tag{21}$$

ϵ labels all the nearest neighbors of the lattice site l and $b_l = e$ $(-e)$ for l denoting the even (odd) sublattice. A more detailed description of the simulation procedure can be found in Ref. [26].

We will first discuss simulations with $\lambda < 1$, where we have a clearly established easy-plane symmetry – we therefore expect that this system allows a good comparison with our analytic results. We will, however, always use values for the parameters for which the out-of-plane vortex is stable [18].

Below T_{KT} we observe two spin wave peaks in $S^{xx}(\mathbf{q},\omega)$, as expected, but only for small $\mathbf{q}$-values, while for large $\mathbf{q}$'s only one peak is visible (the one which is also present in the pure AFM model). Fig. 2 shows simulation results for a 40x40 system with $\lambda = 0.8$ and $e = 0.40$ for two different temperatures, and compares them to the linear spin wave result (which is performed at $T = 0$, but which differs from the finite temperature data only by a T-dependent factor). The ratio of the intensities of the two peaks at comparable $\mathbf{q}$-values is about $\tan^2 \frac{\epsilon}{2}$, as expected from our calculations.

Above T_{KT} the spin wave peaks at finite frequencies vanish as predicted by Nelson and Kosterlitz [25], but we observe now two CP's in $S^{xx}(\mathbf{q},\omega)$, a dominant one at $\mathbf{q} = (\pi,\pi)$ and a smaller one at $\mathbf{q} = (0,0)$ (Fig. 3). Each of them can be fitted very well to the squared Lorentzian (18). By comparing the so obtained intensities $I^x(\mathbf{q})$ and widths $\Gamma^x(\mathbf{q})$ with the theoretical predictions,

$$I^x(\mathbf{q}) = \frac{1}{4\pi} \frac{1}{[1 + (\mathbf{q}\xi)^2]^{\frac{3}{2}}} \tag{22}$$

and

$$\Gamma^x(\mathbf{q}) = \left(\sqrt{2} - 1\right)^{\frac{1}{2}} \frac{\sqrt{\pi}\hat{u}}{2\xi} \sqrt{1 + (\mathbf{q}\xi)^2}, \tag{23}$$

respectively, we find values for the vortex correlation length ξ and the vortex average velocity $\bar{u}$.

The simulations for this temperature range where performed on a 100x100 square lattice with $\lambda = 0.85$ and $e = 0.36$. With this choice of parameters $\tilde{\lambda}$ is about 0.8, i.e. this system is, besides the canting of the spins, formally identical to the pure AFM model as discussed in Ref. [17]. In Table 1 we list the data for ξ and $\bar{u}$ which are obtained by analyzing the width of the CP at $\mathbf{q} = (\pi, \pi)$. The correlation length ξ agrees very well with the Kosterlitz formula [10]

$$\xi(T) = \xi_0 \exp\left(\frac{b}{\sqrt{T/T_{KT} - 1}}\right), \tag{24}$$

in the temperature range 0.83...0.90 with $\xi_0 = 1$, $b \cong 0.61$ and $T_{KT} \cong 0.81$ (Fig. 4); i.e. we find a critical temperature T_{KT} which has about the same value as in the pure AFM model ($T_{KT} \cong 0.79$, [17,18]). For $T \gtrsim 0.9$ the values for ξ no longer fit into this picture and therefore suggest a crossover from the XY-type to a more isotropic behavior of the spins (as was also found for other systems with a rather small easy-plane anisotropy [4,17]). These two regimes can be also observed from the data of the average velocity $\bar{u}$, which decreases monotonically in the temperature range 0.83...0.90, but increases again for $T = 0.95$. The only theory for $\bar{u}$ so far was developed by Huber [27] for the out-of-plane vortices in the pure FM model,

$$\bar{u}_H = \frac{1}{2\xi}\sqrt{\frac{\pi}{2}\ln(4\xi^2 T_{KT})}, \tag{25}$$

and predicts an increasing of $\bar{u}$ with increasing temperature. This is in contrast with our simulation data. However, this is not surprising, because we consider here an AFM with additional Dzyaloshinsky interaction. Nevertheless, we have obtained a similar behavior for $\bar{u}$ (i.e. a decrease of the values of $\bar{u}$ with increasing T) also in the pure AFM and FM models [17]. However, in those cases the variations of $\bar{u}$ for different temperatures was less and the absolute values for $\bar{u}$ were smaller.

The data obtained from analyzing the intensity (22) are listed in Table 2 – the amplitudes and correlation lengths corresponding to the CP at $\mathbf{q} = (\pi, \pi)$ have the subscript π, the others the subscript 0. It appears that the intensity is much more sensitive to the critical regimes than the width: a good XY-like behavior can be observed only for $T = 0.85...0.87$. The temperature $T = 0.83$ seems to be still too close to the Kosterlitz-Thouless transition and the CP at $\mathbf{q} = (0, 0)$ has not yet fully developed as expected from our theory (because its amplitude is smaller than the one for the CP at $T = 0.85$, leading to a different amplitude ratio A_0/A_π). On the other hand, the fitted correlation length jumps to higher values already around $T = 0.9$, suggesting that the crossover regime to the more isotropic behavior extends down to this temperature.

We also see that the data obtained from both of the above CP's does not match completely, as one should expect from Eqn. (17). Table 2 shows that the ratio of the amplitudes A_0/A_π is 0.022...0.024,

which is about 25 percent smaller than we would expect from our theoretical derivation – this yields $A_0/A_\pi = \tan^2 \frac{\xi}{2} \cong 0.03$. This difference is too large to be explained by including the perturbations A and B (16). However, as we have already explained in the previous section, our analytic results were obtained by neglecting any in-plane spin wave contributions – although we expect a sudden softening of the spin stiffness constant at T_{KT}, this is correct only for an infinite system at $\mathbf{q} = (\pi, \pi)$ and $\mathbf{q} = (0, 0)$ [28], but not for $\mathbf{q}$-values away from these points. Having additional intensity from spin waves at finite $[(\pi, \pi) - \mathbf{q}]$ and $\mathbf{q}$ can explain the decrease of the observed amplitude ratio (the intensity of the spin wave peak near $\mathbf{q} = (\pi, \pi)$ is much larger than the intensity of the peak near $\mathbf{q} = (0, 0)$ below T_{KT}) and is probably also responsible for the small difference in the values of ξ_0 and ξ_π.

As for the pure FM and AFM models, we find that the values of ξ obtained from the width and the ones fitted from the intensity do not agree with each other [17,18]. This is probably due to the fact that we assume a dilute gas of freely moving vortices without taking into account the still present in-plane spin wave contributions (see the discussion above), and that we also neglect any interactions with vortex pairs and clusters which can be also found in these systems above T_{KT}. However, from our fits we conclude that these additional interactions will mainly renormalize the vortex parameters rather than changing the functional form of the CP's.

For the out-of-plane correlations we basically observe the same scenario as for the pure AFM model, i.e. below T_{KT} there is a single spin wave peak in $S^{zz}(\mathbf{q}, \omega)$, following the ω_+-dispersion, while above T_{KT} there is an additional CP with maximum intensity and width at $\mathbf{q} = (\pi, \pi)$.

In contrast to the model discussed above, Pomerantz [7] suggested that the in-plane anisotropy of the lipid layer material $Mn(C_{18}H_{35}O_2)_2$ is caused purely by the Dzyaloshinsky interaction. If we simulate an isotropic Heisenberg model (i.e. $\lambda = 1$), but choose the strength of the Dzyaloshinsky interaction as $e = 0.64$, so that $\tilde{\lambda} = 0.8$, then we observe quite a similar dynamical behavior as in the previous case: again we find two CP's above T_{KT} as expected from our vortex gas phenomenology. By fitting the data to our analytic expressions we obtain values for the vortex average velocity $\tilde{u}$ and the vortex correlation length ξ which are slightly smaller than for the model with $\lambda = 0.85$ and $e = 0.36$. However, the ratio ξ_0/ξ_π remains approximately the same. This indicates that the dynamics of the system as revealed by the correlation functions is qualitatively the same for the two sets of parameters, while there are small quantitative differences.

In view of the above results, we expect that $Mn(C_{18}H_{35}O_2)_2$ will have vortices as fundamental magnetic excitations. However, if Pomerantz' suggestion is correct, it would mean that because of the small easy-plane character ($\lambda = 1$, $e \cong 0.064$, leading to $\tilde{\lambda} \cong 0.998$) the crossover from planar to isotropic behavior would occur at a temperature $T_2 \cong 0.835 \equiv 1.52K$ (i.e. $\xi(T_2) \cong (1 - \tilde{\lambda})^{-1/2}$ [4]) which is very close to the

Kosterlitz-Thouless temperature $T_{KT} \cong 0.81 \equiv 1.47K$. On the other hand, in the low temperature regime the small easy-axis anisotropy will dominate leading to an Ising-like spin dynamics with an ordered phase below $T \cong 0.5K$ [7,8,9].

4 Summary

In this manuscript we have discussed the spin dynamics of an easy-plane AFM Heisenberg model with additional Dzyaloshinsky interaction. We were able to show that the combined Hamiltonian can be mapped onto a Hamiltonian for a pure AFM Heisenberg model with appropriate renormalized parameters and rotated spins. The rotation points, for neighboring spins on different sublattices, in the same direction and, thus, leads to a local ferromagnetic moment. This canting accounts for the presence of a second spin wave peak in the dynamical correlation function below the Kosterlitz-Thouless transition temperature T_{KT}. Above T_{KT} we can also observe an additional CP at $\mathbf{q} = (0,0)$ due to this uniform canting of the spins. Our theoretical predictions were qualitatively confirmed by numerical MC-MD simulations. However, a quantitative comparison, especially of the data obtained by fitting the intensity (which reflects static properties) and the width (which reflects dynamic properties of the system), revealed that our vortex gas ansatz is too simple and should be extended, probably by including interactions with the remaining in-plane spin waves and with vortex pairs and clusters.

Because the Dzyaloshinsky interaction enhances the easy-plane character of a system, we observe planar spin dynamics even in an isotropic Heisenberg model, if we add this antisymmetric exchange interaction. This fact implies that the lipid layer material $Mn(C_{18}H_{35}O_2)_2$, even if it is described by an isotropic Heisenberg model with additional Dzyaloshinsky interaction, might serve as a literally 2d magnetic material with planar spin dynamics. However, due to the small value of the anisotropic exchange interaction and the additional weak easy-axis anisotropy, as suggested by Pomerantz [7], there would be only a limited temperature regime, where typical 2d easy-plane spin dynamics, and especially vortex dynamics, could be observed: at low temperatures we would expect that the system will exhibit Ising-like behavior, while for temperatures just above T_{KT} there would be a crossover to isotropic spin dynamics. More experiments at low temperatures would certainly help to form a better understanding of the spin dynamics in $Mn(C_{18}H_{35}O_2)_2$.

Acknowledgements

This work was supported by Deutsche Forschungsgemeinschaft (Project No. C19, SFB 213), by NATO (Collaborative Research Grant No. 0013/89), and by the United States Department of Energy.

Figure Captions

1. In-plane structure of a single static vortex for $\lambda = 0.85$ and $e = 0.36$; the arrows show the projection of the spins onto the xy-plane; solid (dashed) arrows indicate a positive (negative) z-component of the corresponding spin. All the spins are rotated away from the vortex core by the same canting angle $\frac{1}{2}\arctan(e) = 17.28$.

2. Spin wave dispersions as seen in the in-plane correlation function; $+$, $*$: $T = 0.3$; $\diamond$, $\triangle$: $T = 0.5$; solid and dashed line: linear theory for $T = 0$.

3. Vortex CP's in $S^{xx}(\mathbf{q},\omega)$ for a system with $\lambda = 0.85$ and $e = 0.36$ at $T = 0.86$ near the AFM (a) and the FM (b) Bragg point; ——: numerical data; - - -: fit to Eqn. (18).

4. Correlation length as function of temperature; $\diamond$: simulation data (obtaind by fitting the width of $S^{xx}(\mathbf{q},\omega)$); ——: fit to Eqn. (24). The dashed line indicates the critical temperature $T_{KT} = 0.81$.

References

[1] de Jongh L. J.: *Magnetic Properties of Layered Transition Metal Compounds.* Kluwer Academic Publisher. 1990.

[2] Regnault L. P.; Lartigue C.; Legrand J. F.; Farago B.; Rossat-Mignot J.; Henry J. Y.: *Physica* **B156-157** (1989) 298.

[3] Gaveau P.;. Boucher J. P, Regnault L. P.; Henry J. Y.: *J. Appl. Phys.* **69(27)** (1991) 6228.

[4] Hirakawa K.; Yoshizawa H.; Ubokoshi K.: *J. Phys. Soc. Japan.* **51** (1982) 2151.

[5] Aïn M.: *J. Physique* **48** (1987) 2103.

[6] Wiesler D. G.; Zabel H.; Shapiro S. M.: *Physica* **B156-157** (1989) 292.

[7] Pomerantz M.: *Surface Science* **142** (1984) 556.

[8] Haseda T.; Yamakawa H.; Ishizuka M.; Okuda Y.; Kubota T.; Hata M.; Amaya K.: *Solid State Commun.* **24** (1977) 599.

[9] Head D. I.; Blott B. H.; Melville D.: *J. Physique* **C8** (1988) 1649.

[10] Kosterlitz J. M .; Thouless D. J.: *J. Phys* **C6** (1973) 1181.

[11] Berezinsky V. L.: *Sov. Phys. JETP* **34** (1972) 610.

[12] Mertens F. G.; Bishop A. R.; Wysin G. M.; Kawabata C.: *Phys. Rev. Lett.* **59** (1987) 117.

[13] Mertens F. G.; Bishop A. R.; Wysin G. M.; Kawabata C.: *Phys. Rev.* **B39** (1989) 591.

[14] Gouvêa M. E.; Wysin G. M.; Bishop A. R.; Mertens F. G.: *Phys. Rev.* **B39** (1989) 11840.

[15] Gouvêa M. E.; Wysin G. M.; Bishop A. R.; Mertens F. G.: *J. Phys. Condens. Matter* **1** (1989) 4387.

[16] Gouvêa M. E.; Mertens F. G.; Bishop A. R.; Wysin G. M.: *J. Phys. Condens. Matter* **2** (1990) 1853.

[17] Völkel A. R.; Bishop A. R.; Mertens F. G.; Wysin G. M.: *J. Phys.: Condensed Matter*, in press (1992).

[18] Völkel A. R.; Wysin G. M.; Bishop A. R.; Mertens F. G.: *Phys. Rev.* **B44** (1991) 10066.

[19] Richards P. M .; Salamon M. B.: *Phys. Rev.* **B9** (1974) 32.

[20] Yoshida H .; Saiki K.: *J. Phys. Soc. Japan* **33** (1972) 1566.

[21] Dzyaloshinsky I.: *J. Phys. Chem. Solids* **4** (1958) 241.

[22] Moriya T.: *Phys. Rev.* **120** (1960) 91.

[23] Holstein T .; Primakoff H.: *Phys. Rev.* **58** (1940) 1098.

[24] Mikeska H. J.: *J. Phys. C* **13** (1980) 2913.

[25] Nelson D. R .; Kosterlitz J. M.: *Phys. Rev. Lett.* **39** (1977) 1201.

[26] Wysin G. M .; Bishop A. R.: *Phys. Rev.* **B42** (1990) 810.

[27] Huber D. L.: *Phys. Rev.* **B26** (1982) 3758.

[28] Bramwell S. T .; Holdsworth P. C. W.: *preprint.*

T	ξ	$\tilde{u}$
0.83	32.50	2.27
0.85	14.29	1.33
0.86	9.88	1.26
0.87	8.19	1.23
0.90	4.96	0.97
0.95	6.04	1.45

Table 1: Data for ξ and $\tilde{u}$ obtained by analyzing the width of the CP at $\mathbf{q} = (\pi, \pi)$ in $S^{xx}(\mathbf{q}, \omega)$

	$\mathbf{q} = (\pi, \pi)$		$\mathbf{q} = (0, 0)$			
T	ξ_π	A_π	ξ_0	A_0	$\frac{\xi_0}{\xi_\pi}$	$\frac{A_0}{A_\pi}$
0.83	4.56	0.69	4.25	0.0117	0.93	0.017
0.85	5.05	0.58	4.70	0.0141	0.93	0.024
0.86	3.86	0.45	3.64	0.0089	0.94	0.020
0.87	3.73	0.41	3.46	0.0090	0.93	0.022
0.90	3.97	0.33	3.61	0.0074	0.98	0.022
0.95	2.12	0.16	2.96	0.0037	1.40	0.023

Table 2: Data as obtained by analyzing the intensities of the two CP's in $S^{xx}(\mathbf{q}, \omega)$

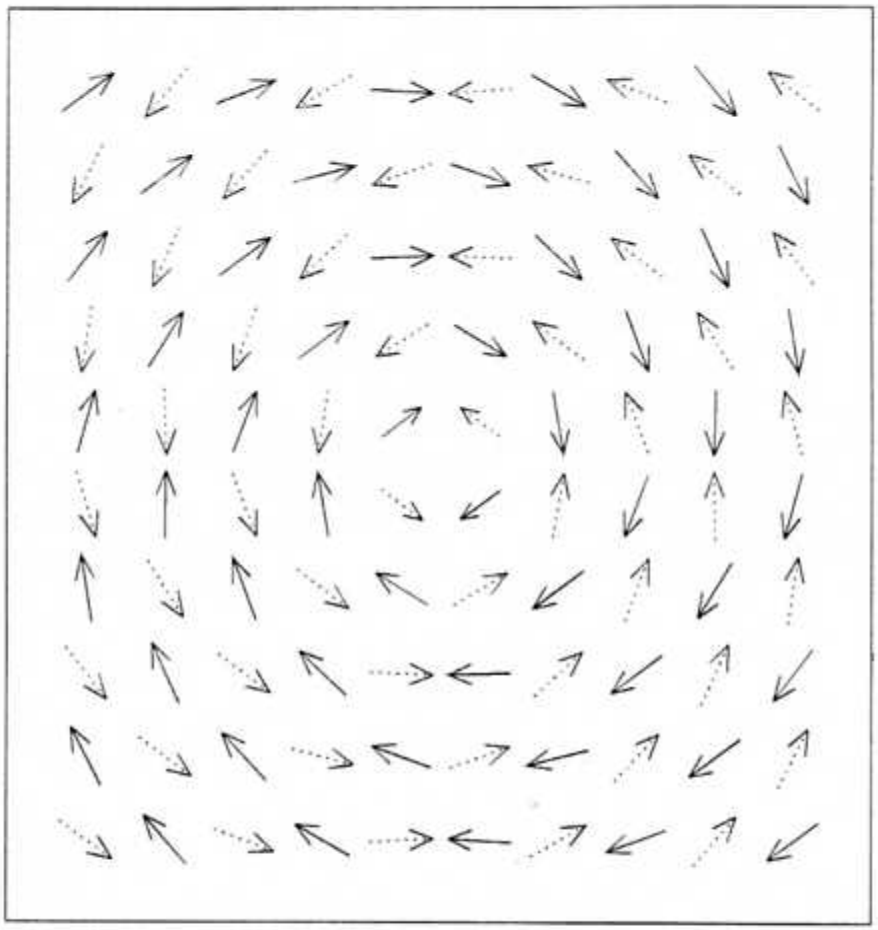

FIG. 1.

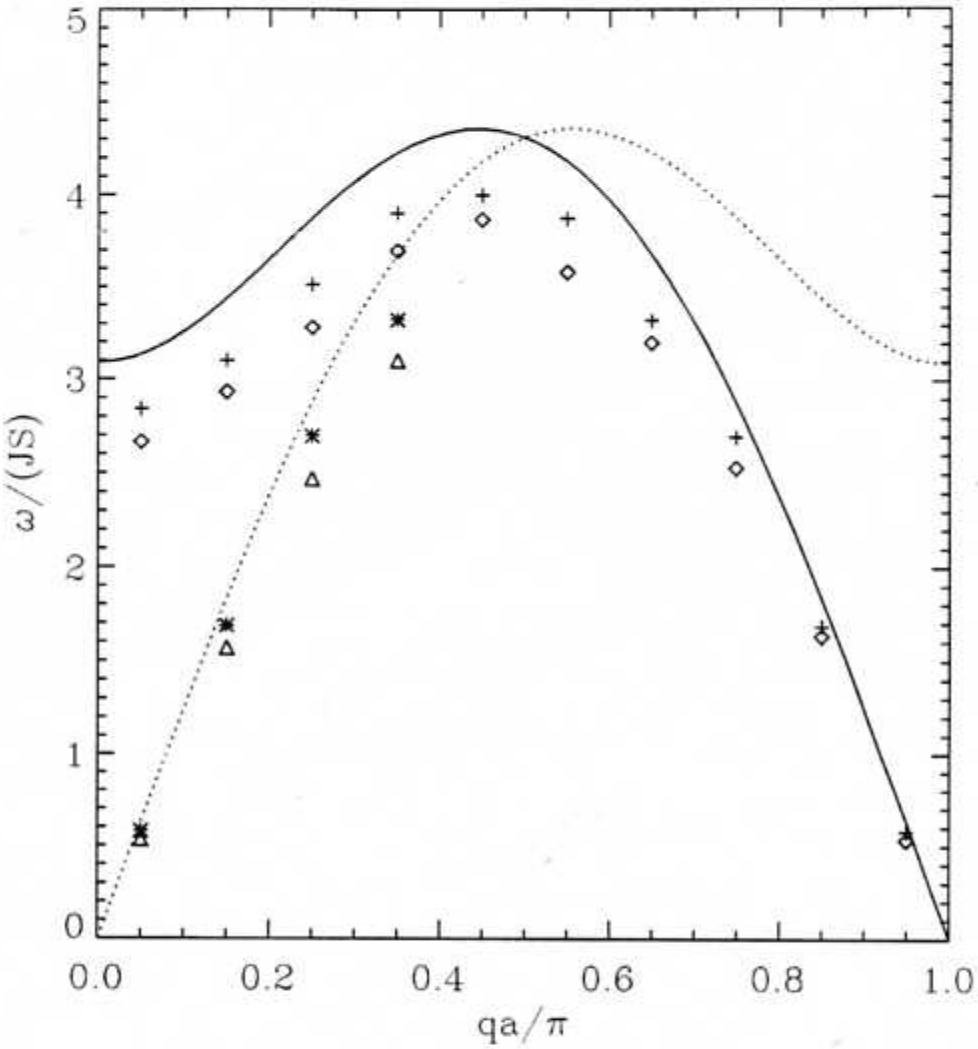

FIG. 2.

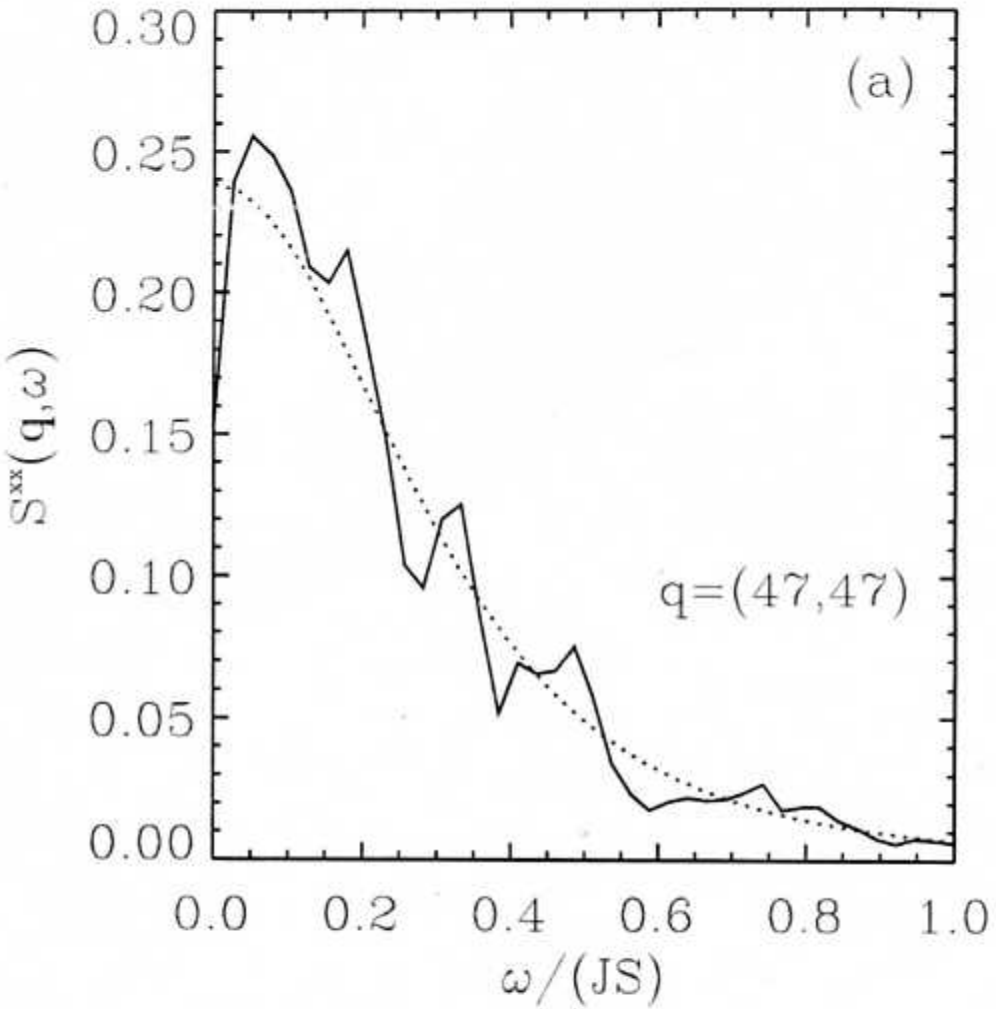
0.30
0.25
0.20
0.15
0.10
0.05
0.00
0.0
0.2
0.4
0.6
0.8
1.0
(a)
q=(47,47)
$S^{xx}(q,\omega)$
$\omega/(JS)$

FIG. 3 a.

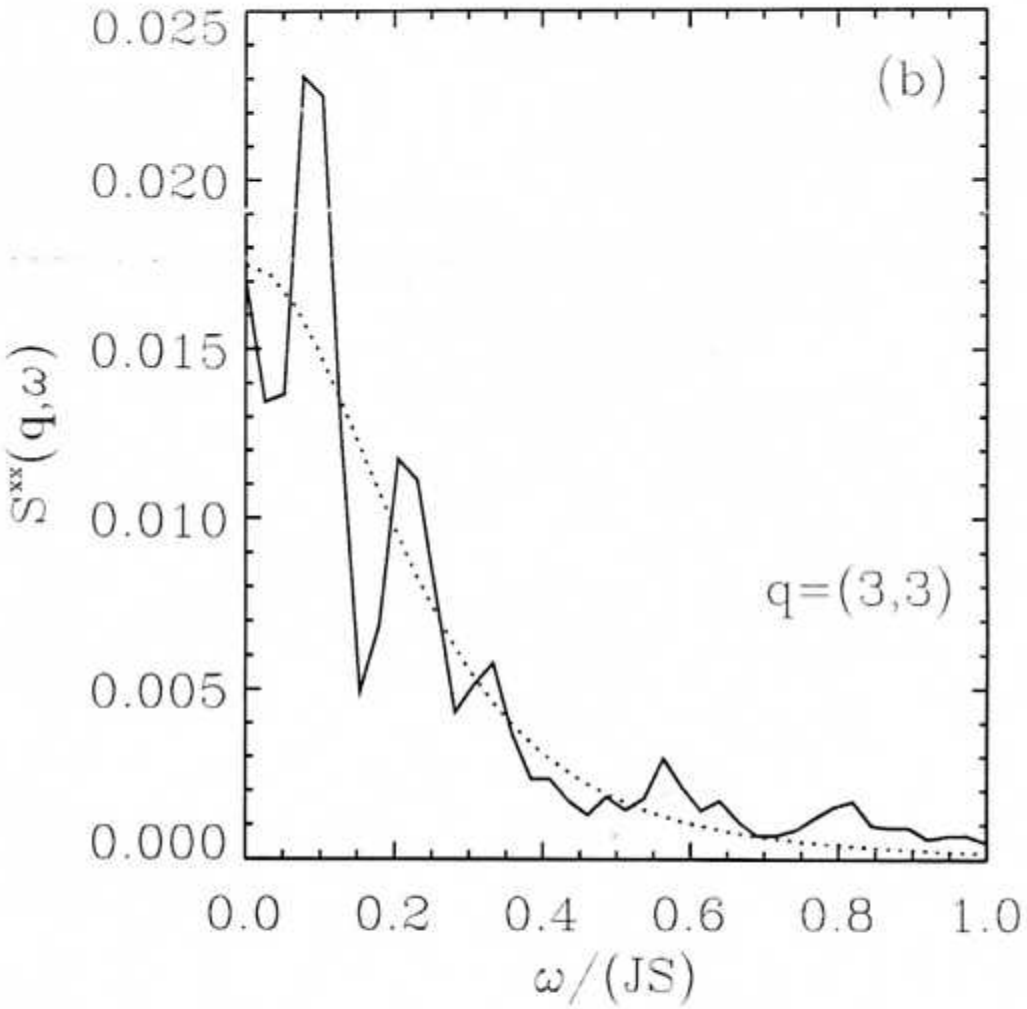
0.025
0.020
0.015
0.010
0.005
0.000
(b)
q=(3,3)
$S^{xx}(q,\omega)$
0.0
0.2
0.4
0.6
0.8
1.0
$\omega/(JS)$

FIG. 3b.

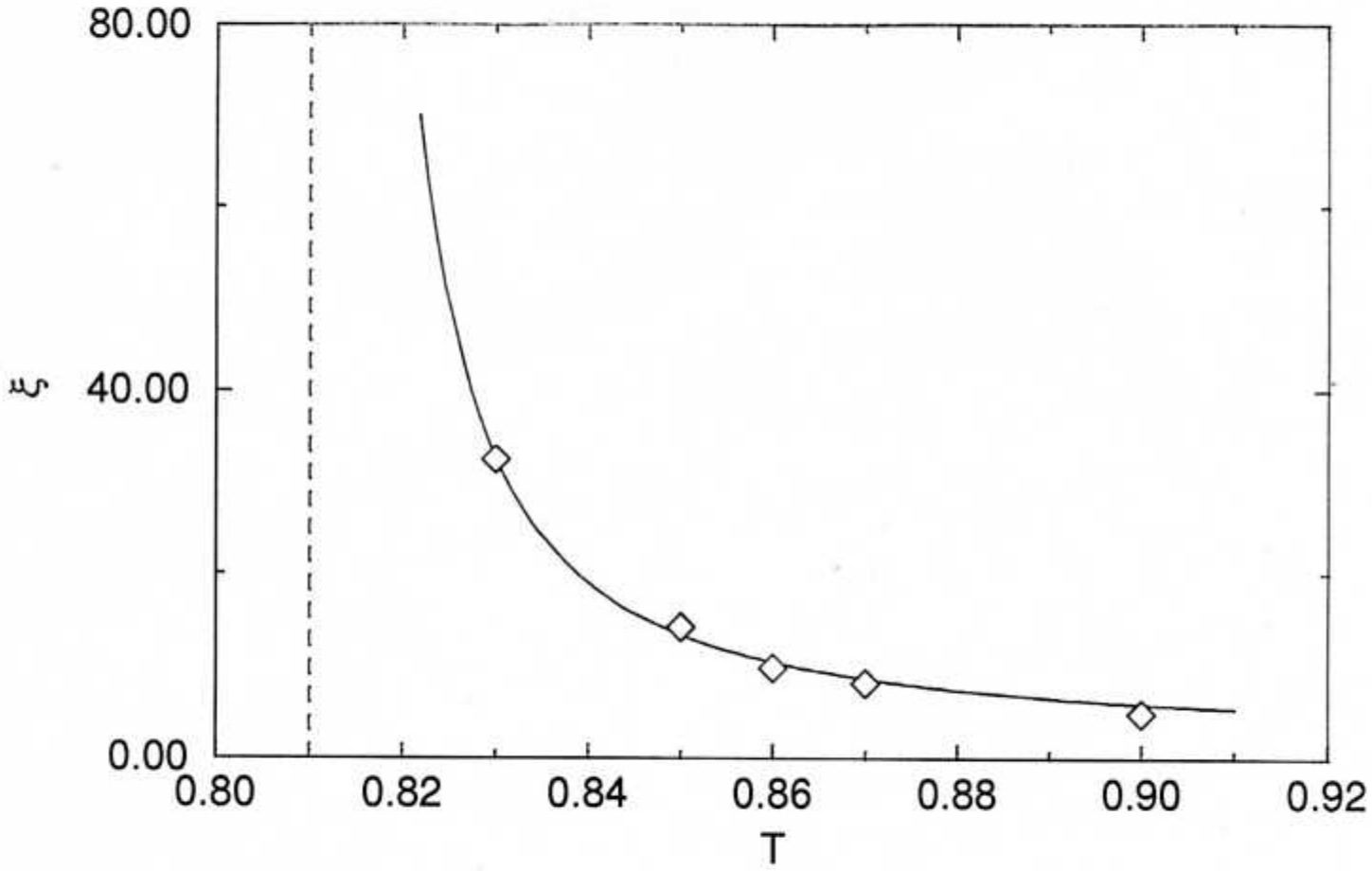

FIG. 4.